Biochimica et Biophysica Acta 1822 (2012) 1826–1836

Contents lists available at SciVerse ScienceDirect

Biochimica et Biophysica Acta

journal homepage: www.elsevier.com/locate/bbadis

Autophagy-dependent and -independent involvement of AMP-activated protein kinase in 6-hydroxydopamine toxicity to SH-SY5Y neuroblastoma cells

Katarina Arsikin [a], Tamara Kravic-Stevovic [b], Maja Jovanovic [c], Biljana Ristic [a], Gordana Tovilovic [d], Nevena Zogovic [d], Vladimir Bumbasirevic [b], Vladimir Trajkovic [a,*], Ljubica Harhaji-Trajkovic [d,*]

[a] Institute of Microbiology and Immunology, School of Medicine, University of Belgrade, Dr. Subotica 1, 11000 Belgrade, Serbia
[b] Institute of Histology and Embryology, School of Medicine, University of Belgrade, Belgrade, Serbia
[c] Institute of Biochemistry, School of Medicine, University of Belgrade, Belgrade, Serbia
[d] Institute for Biological Research, University of Belgrade, Belgrade, Serbia

ARTICLE INFO

Article history:
Received 4 May 2012
Received in revised form 7 August 2012
Accepted 8 August 2012
Available online 16 August 2012

Keywords:
6-Hydroxydopamine
Neurotoxicity
AMPK
Autophagy
p38
Oxidative stress

ABSTRACT

The role of the main intracellular energy sensor adenosine monophosphate (AMP)-activated protein kinase (AMPK) in the induction of autophagic response and cell death was investigated in SH-SY5Y human neuroblastoma cells exposed to the dopaminergic neurotoxin 6-hydroxydopamine (6-OHDA). The induction of autophagy in SH-SY5Y cells was demonstrated by acridine orange staining of intracellular acidic vesicles, the presence of autophagosome- and autophagolysosome-like vesicles confirmed by transmission electron microscopy, as well as by microtubule-associated protein 1 light-chain 3 (LC3) conversion and p62 degradation detected by immunoblotting. 6-OHDA induced phosphorylation of AMPK and its target Raptor, followed by the dephosphorylation of the major autophagy inhibitor mammalian target of rapamycin (mTOR) and its substrate p70S6 kinase (S6K). 6-OHDA treatment failed to suppress mTOR/S6K phosphorylation and to increase LC3 conversion, p62 degradation and cytoplasmatic acidification in neuroblastoma cells in which AMPK expression was downregulated by RNA interference. Transfection of SH-SY5Y cells with AMPK or LC3β shRNA, as well as treatment with pharmacological autophagy inhibitors suppressed, while mTOR inhibitor rapamycin potentiated 6-OHDA-induced oxidative stress and apoptotic cell death. 6-OHDA induced phosphorylation of p38 mitogen-activated protein (MAP) kinase in an AMPK-dependent manner, and pharmacological inhibition of p38 MAP kinase reduced neurotoxicity, but not AMPK activation and autophagy triggered by 6-OHDA. Finally, the antioxidant N-acetyl cysteine antagonized 6-OHDA-induced activation of AMPK, p38 and autophagy. These data suggest that oxidative stress-mediated AMPK/mTOR-dependent autophagy and AMPK/p38-dependent apoptosis could be valid therapeutic targets for neuroprotection.

1. Introduction

Parkinson's disease (PD) is a neurodegenerative disorder characterized by the preferential loss of the dopaminergic neurons of the substantia nigra, part of the brain that controls muscle movement, resulting in bradykinesia, rigidity and resting tremors [1]. Even though the neurochemical defects and neuropathological characteristics of this disease are well defined, its etiology is still unknown. One of the most common neurotoxins used to selectively kill dopaminergic and noradrenergic neurons in experimental models of PD both in vivo and in vitro is oxidopamine, also known as 6-hydroxydopamine (6-OHDA) [2]. 6-OHDA is a hydroxylated analogue of the natural neurotransmitter dopamine, and its presence has been demonstrated in both rat and human brain [3,4]. Neurotoxic action of oxidopamine is mainly mediated by reactive oxygen species (ROS) such as hydrogen peroxide, superoxide and hydroxyl radicals generated by its intra or extracellular auto-oxidation [5]. Hydrogen peroxide, which is also generated by monoamine oxidase activity in 6-OHDA treated neurons, further reacts with iron and produces highly reactive hydroxyl radical [2]. The oxidative stress induces lipid peroxidation, cytoskeleton disorganization and DNA defects, which together with the direct inhibition of the mitochondrial respiratory chain by 6-OHDA eventually results in apoptotic and/or necrotic neuronal cell death [2].

Macroautophagy (referred to hereafter as autophagy) is a catabolic process involving the degradation of the cell's own components in organelles called autophagolysosomes [6]. It begins with the

Abbreviations: 6-OHDA, 6-hydroxydopamine; AMPK, AMP-activated protein kinase; DHE, dihydroethidium; DHR, dihydrorhodamine; ERK, extracellular signal-regulated kinase; FACS, fluorescence-activated cell sorting; FITC, fluorescein isothiocyanate; LC3, microtubule-associated protein 1 light-chain 3; LDH, lactate dehydrogenase; MAPK, mitogen-activated protein kinase; mTOR, mammalian target of rapamycin; MTT, 3-(4,5-dimethylthiazol-2-yl)-2,5-diphenyltetrazolium bromide; PD, Parkinson's disease; PI, propidium iodide; ROS, reactive oxygen species; S6K, p70S6 kinase; shRNA, short hairpin RNA; TEM, transmission electron microscopy

* Corresponding authors. Tel.: +381 11 3643 233; fax: +381 11 3643 235.
E-mail addresses: vtrajkovic@med.bg.ac.rs (V. Trajkovic), buajk@yahoo.com (L. Harhaji-Trajkovic).

0925-4439/$ – see front matter © 2012 Elsevier B.V. All rights reserved.
doi:10.1016/j.bbadis.2012.08.006

sequestration of intracellular content in double-membraned autophagosomes, followed by their fusion with lysosomes and formation of autophagolysosomes, in which the internal content is degraded by acidic lysosomal hydrolases. While the physiological role of autophagy is to eliminate unused long-lived proteins and damaged organelles, it also acts as a survival mechanism in metabolic or hypoxic stress [7]. On the other hand, when it is extensive, activated inappropriately or in cells which are unable to die by apoptosis, it can function as an alternative cell-death pathway (programmed cell death type II) [8–10]. Accordingly, it has been proposed that autophagy is involved in the maintenance of neuronal homeostasis, with either defective or excessive autophagy contributing to the neuronal loss in ischemic brain injury and neurodegenerative disorders, including PD [11,12]. The expression and activation of numerous Atg proteins required for autophagic response are suppressed by mammalian target of rapamycin (mTOR), a serine/threonine kinase that acts as a major negative regulator of autophagy [13,14]. One of the principal regulators of mTOR activation is AMP-activated protein kinase (AMPK), the main energy-saving intracellular enzyme activated in various stress conditions by the increase in AMP/ATP ratio [15]. AMPK-mediated phosphorylation of its target Raptor and consequent inhibition of mTOR induce autophagy [16], causing either cytotoxicity or cytoprotection in a context-dependent manner [17–20]. AMPK-dependent autophagy might play a dual role also in the neuronal survival, being neuroprotective in amyloid-beta accumulation [21] and deleterious in tributyltin chloride neurotoxicity [22].

Oxidopamine has been found to induce autophagy in neurons both in vitro and in vivo [23–27], and it seems that autophagy might be involved in 6-OHDA-induced neuronal damage in vivo [25,27]. However, the mechanisms underlying these phenomena have not been extensively elucidated. More specifically, no study to our knowledge has examined the role of AMPK/mTOR signaling axis in 6-OHDA-triggered neuronal autophagy and neurotoxicity. In the present study, we investigate in more detail the role of the AMPK/mTOR signaling pathway in 6-OHDA-induced autophagy in SH-SY5Y neuron-like cells, as well as the contribution of the autophagic response to the in vitro neurotoxicity of 6-OHDA.

2. Materials and methods

2.1. Cells and reagents

All reagents were purchased from Sigma (St. Louis, MO), unless stated otherwise. The human neuroblastoma cell line SH-SY5Y (American Type Culture Collection) was grown at 37 °C in a humidified atmosphere with 5% CO_2, in a Modified Eagle Medium + F12 cell culture medium (1:1) (PAA Laboratories, Pasching, Austria) supplemented with 10% fetal calf serum, 2 mM L-glutamine, nonessential amino acids and penicillin/streptomycin. The cells were prepared for experiments using the conventional trypsinization procedure with trypsin/EDTA and incubated in 96-well flat-bottom plates (1.5×10^4 cells/well) for the cell viability assessment, 24-well plates (1.2×10^5 cells/well) for the flow cytometric analysis, or 60 mm cell culture plates (1×10^6 cells) for the Western blotting. Cells were rested for 24 h and then treated with 6-OHDA in the absence or presence of the antioxidant N-acetylcysteine, mTOR inhibitor rapamycin, p38 inhibitor SB203580 or the autophagy inhibitors bafilomycin A1, chloroquine, NH_4Cl, 3-methyladenine and wortmannin, as described in Results and figure legends.

2.2. Cell viability assays

Crystal violet staining of adherent, viable cells, measurement of mitochondria-dependent reduction of 3-(4,5-dimethylthiazol-2-yl)-2, 5-diphenyltetrazolium bromide (MTT) to formazan as an indicator of the mitochondrial dehydrogenase activity, and the release of intracellular enzyme lactate dehydrogenase (LDH) as a marker of cell membrane damage, were used to determine cell viability exactly as previously described [28]. The results were presented as % of the crystal violet/MTT absorbance obtained in untreated cells (100%). The percentage of dead cells was determined by LDH assay using the following formula: $[(E-C)/(T-C)]\times100$, where E is the experimental absorbance of treated cells, C is the control absorbance of untreated cells, and T is the absorbance corresponding to the maximal (100%) LDH release of Triton X-100-lysed cells.

2.3. Apoptosis analysis and caspase activation

Apoptotic cell death was analyzed by double staining with annexin V-FITC and PI, in which annexin V binds to early apoptotic cells with exposed phosphatidylserine, while PI labels the late apoptotic/necrotic cells with membrane damage. Staining was performed according to the instructions by the manufacturer (BD Pharmingen, San Diego, CA). A green/red (FL1/FL2) fluorescence of annexin/PI^- and PI-stained cells was analyzed with FACSCalibur flow cytometer (BD, Heidelberg, Germany). The numbers of viable (annexin$^-$/PI^-), apoptotic (annexin$^+$/PI^-) and late apoptotic/necrotic (annexin$^+$/PI^+) cells were determined with a Cell Quest Pro software (BD). Activation of caspases was measured by flow cytometry after labeling the cells with a cell-permeable, FITC-conjugated pan-caspase inhibitor (ApoStat; R&D Systems, Minneapolis, MN) according to the manufacturer's instructions. The increase in green fluorescence (FL1) as a measure of caspase activity was determined using FACSCalibur flow cytometer.

2.4. Reactive oxygen species (ROS) determination

Intracellular production of ROS was determined by measuring the intensity of green fluorescence emitted by the redox-sensitive dye dihydrorhodamine 123 (DHR; Invitrogen, Paisley, UK). The production of superoxide was measured using superoxide-selective fluorochrome dihydroethidium (DHE; Invitrogen, Paisley, UK). DHR (2 μM) was added to cell cultures at the beginning of treatment, while DHE (20 μM) was incubated with the cells for the last 30 min of the treatment. At the end of incubation, cells were detached by trypsinization, washed in PBS, and the mean intensity of green (FL1, DHR) or red (FL2, DHE) fluorescence, corresponding to total ROS or superoxide levels, respectively, was determined using a FACSCalibur flow cytometer.

2.5. Intracellular detection of acidic vesicles and autophagic vacuoles

The acidic vesicles were visualized by acridine orange staining. After incubation, cells were washed with PBS and stained with acridine orange (1 μM) for 15 min at 37 °C. Subsequently, cells were washed and analyzed under the inverted fluorescent microscope. Autophagolysosomes and lysosomes appeared as red fluorescent cytoplasmic vesicles, while nuclei were stained green. Alternatively, acridine orange-stained cells were trypsinized, washed and analyzed on a FACSCalibur flow cytometer using Cell Quest Pro software. Accumulation of acidic vesicles was quantified as red/green fluorescence ratio (mean FL3/FL1). The presence of double-membraned autophagosomes was evaluated by transmission electron microscopy (TEM). The trypsinized cells were fixed with 2.5% glutaraldehyde in PBS, followed by 2% OsO_4. After dehydration, thin sections were stained with uranyl acetate and lead citrate for observation under a Morgagni 268(D) electron microscope (FEI, Hillsboro, OR).

2.6. Immunoblot analysis

The cells were lysed in lysis buffer (30 mM Tris–HCl pH 8.0, 150 mM NaCl, 1% NP-40, 1 mM phenylmethylsulfonylfluoride and protease inhibitor cocktail) on ice for 30 min, centrifuged at 14000 g for 15 min at 4 °C, and the supernatants were collected. Equal amounts of protein from each sample were separated by SDS-PAGE and transferred to

nitrocellulose membranes (Bio-Rad, Marnes-la-Coquette, France). Following incubation with antibodies against microtubule-associated protein 1 light-chain 3β (LC3β), p62, phospho-AMPKα (Thr172), AMPKα, phospho-Raptor (Ser792), Raptor, phospho-mTOR (Ser2448), mTOR, phospho-p70S6K (Thr389), p70S6K, phospho-p38 (Thr180/Tyr182), p38, beclin-1, and β-actin (Cell Signaling Technology, Beverly, MA) as primary antibodies and peroxidase-conjugated goat anti-rabbit IgG (Jackson IP Laboratories, West Grove, PA) as a secondary antibody, specific protein bands were visualized using enhanced chemiluminescence reagents for Western blot analysis (Amersham Pharmacia Biotech, Piscataway, NJ). The protein levels were quantified by densitometry using ImageJ software and expressed relative to actin (LC3-II, beclin-1, p62) or corresponding total protein signals (phospho-AMPK, phospho-mTOR, phospho-Raptor, phospho-p70S6K, phospho-p38). The results are presented as the fold change in signal intensity compared to that of the untreated control at the same time-point, which was arbitrarily set to 1.

2.7. RNA interference

The short hairpin RNA (shRNA) targeting human LC3β or AMPKα 1/2 genes, as well as scrambled control shRNA were obtained from Santa Cruz Biotechnology (Santa Cruz, CA). SH-SY5Y cells in 6 well plates were transfected with LC3β, AMPK or control shRNA according to the manufacturer's protocol, using shRNA Plasmid Transfection Reagent and Medium (Santa Cruz Biotechnology, Santa Cruz, CA). The stably transfected cells were selected as recommended by the manufacturer and maintained in selection medium containing puromycin (10 μg/ml). Only the cells that have been propagated for less than eight passages were used in the experiments.

2.8. Statistical analysis

The statistical significance of the differences was analyzed by one-way analysis of variance (ANOVA) followed by Student–Newman–

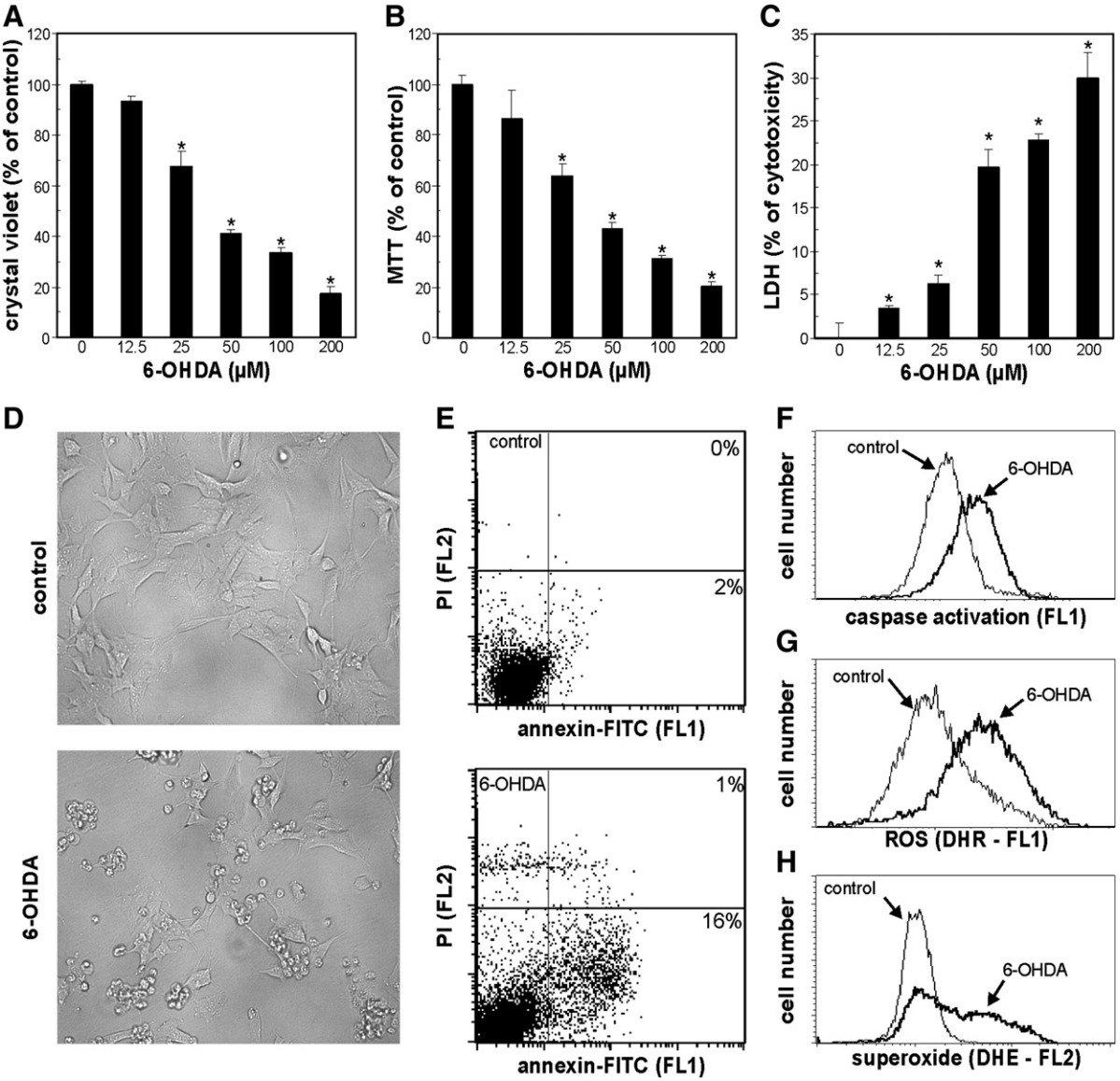

Fig 1. 6-Hydroxydopamine-induced apoptosis in SH-SY5Y cells is associated with oxidative stress and caspase activation. (A–C) SH-SY5Y cells were incubated in the presence of different concentrations of 6-OHDA and cell viability was determined after 24 h by crystal violet (A), MTT (B) and LDH test (C). (D–H) SH-SY5Y cells were incubated with 6-OHDA (50 μM) and cell morphology was examined by inverted microscopy after 24 h (D). Alternatively, after 16 h of incubation cells were stained with annexin V-FITC/PI (E), ApoStat (F), DHR (G) or DHE (H) and proportion of apoptotic (annexin$^+$/PI$^-$) cells (E), caspase activation (F), ROS (G) or superoxide (H) production was examined by flow cytometry. The representative dot plots and histograms from at least three experiments are presented. The data are mean ± SD values of triplicate measurements from a representative of three experiments (*$p<0.05$ vs. untreated cells).

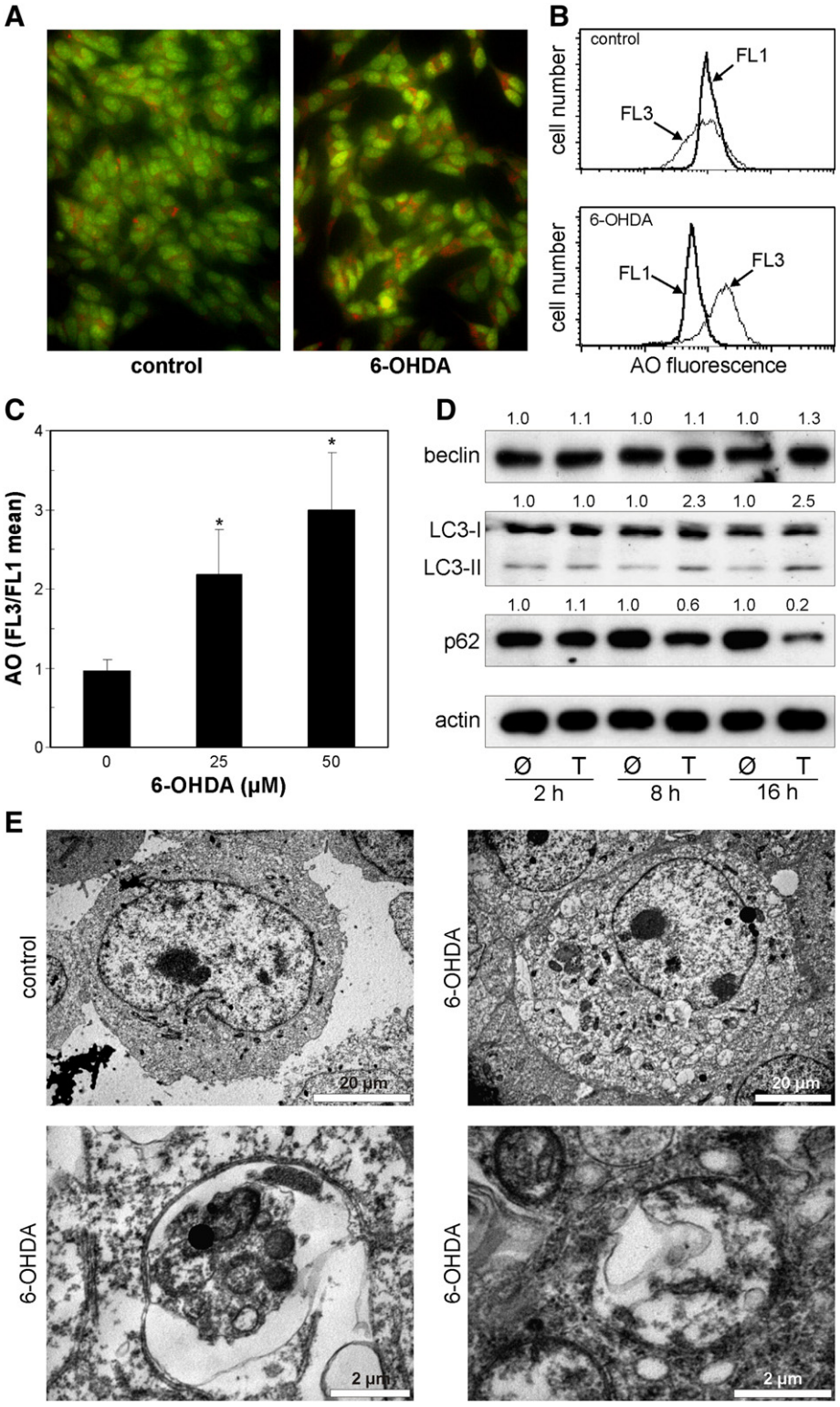

Fig. 2. 6-OHDA induces autophagy in SH-SY5Y cells. (A–C) SH-SY5Y cells were incubated for 16 h in the presence of 50 μM (A, B) or different concentrations of 6-OHDA (C). The presence of acridine orange (AO)-stained intracellular vesicles was demonstrated by fluorescent microscopy (A) and flow cytometry, showing an increase in red-to-green (FL3/FL1) mean fluorescence intensity (B, C). The data in (C) are mean ± SD values from three independent experiments (*$p<0.05$ vs. untreated cells). (D) LC3 conversion, beclin-1 and p62 levels in SH-SY5Y cells treated with 6-OHDA (50 μM) were assessed by immunoblotting at the indicated time points. The blots from a representative of three experiments are presented with the densitometry data above the relevant bands. (E) The TEM analysis of cells treated with 6-OHDA (50 μM) for 16 h showing intensive vacuolization (upper right panel), double-membraned autophagosomes (lower left) and single-membraned autophagolysosomes containing cellular components (lower right).

Keuls test. A p value less than 0.05 was considered statistically significant.

3. Results

3.1. 6-Hydroxydopamine induces oxidative stress-mediated apoptotic death of SH-SY5Y cells

The treatment with 6-OHDA for 24 h in a dose-dependent manner reduced the viability of SH-SY5Y cells, as demonstrated by measuring cell numbers, mitochondrial dehydrogenase activity and cell membrane damage by crystal violet, MTT and LDH test, respectively (Fig. 1A–C). The IC_{50} concentration was approximately 50 μM based on MTT and crystal violet data, so this dose was chosen for further experiments. Consistent with the induction of cell death, cells treated with 6-OHDA lost their processes, became round, smaller and detached from the culture well surface (Fig. 1D). The flow cytometric analysis of the cells stained with annexin V-FITC and propidium iodide has demonstrated that 6-OHDA induced a significant increase in numbers of early apoptotic cells with intact cell membrane (annexin$^+$/PI$^-$), and only a marginal increase in numbers of late apoptotic/necrotic cells (annexin$^+$/PI$^+$) (Fig. 1E). 6-OHDA mediated apoptosis was associated with activation of caspases, the principal apoptosis-executing enzymes (Fig. 1F). The staining with the redox-sensitive fluorochrome DHR and the superoxide-selective DHE revealed that oxidopamine induced oxidative stress, which could be at least partly attributed to the superoxide production (Fig. 1G, H). Therefore, 6-OHDA induces oxidative stress and caspase-dependent apoptosis in SH-SY5Y cells.

3.2. 6-Hydroxydopamine induces autophagy in SH-SY5Y cells

We next explored the ability of 6-OHDA to induce autophagy in SH-SY5Y cells. Both fluorescent microscopy and flow cytometry demonstrated an increase in acridine orange red fluorescence in 6-OHDA-treated SH-SY5Y cells (Fig. 2A–C), indicating the presence of intracellular acidification as one of the hallmarks of autophagic response. Accordingly, immunoblot analysis revealed that 6-OHDA in a time-dependent manner increased the conversion of LC3-I protein to its lipidated, autophagosome-associated LC3-II form, while the expression of proautophagic protein beclin-1 was only slightly upregulated (Fig. 2D). The apparently low degree of LC3 conversion upon 6-OHDA treatment was probably due to the fact that LC3-II increase is counteracted by its simultaneous degradation in autophagolysosomes, and does not always directly correspond to the extent of the autophagy induction [29]. However, the treatment with oxidopamine markedly decreased the level of p62, a selective target for autophagic degradation [30], thus confirming the increase in autophagy-mediated proteolysis (Fig. 2D). Finally, the induction of autophagy was confirmed by ultrastructural TEM analysis, showing extensive cytoplasmic vacuolization with many double-membraned autophagosomes and single-membraned autolysosome-

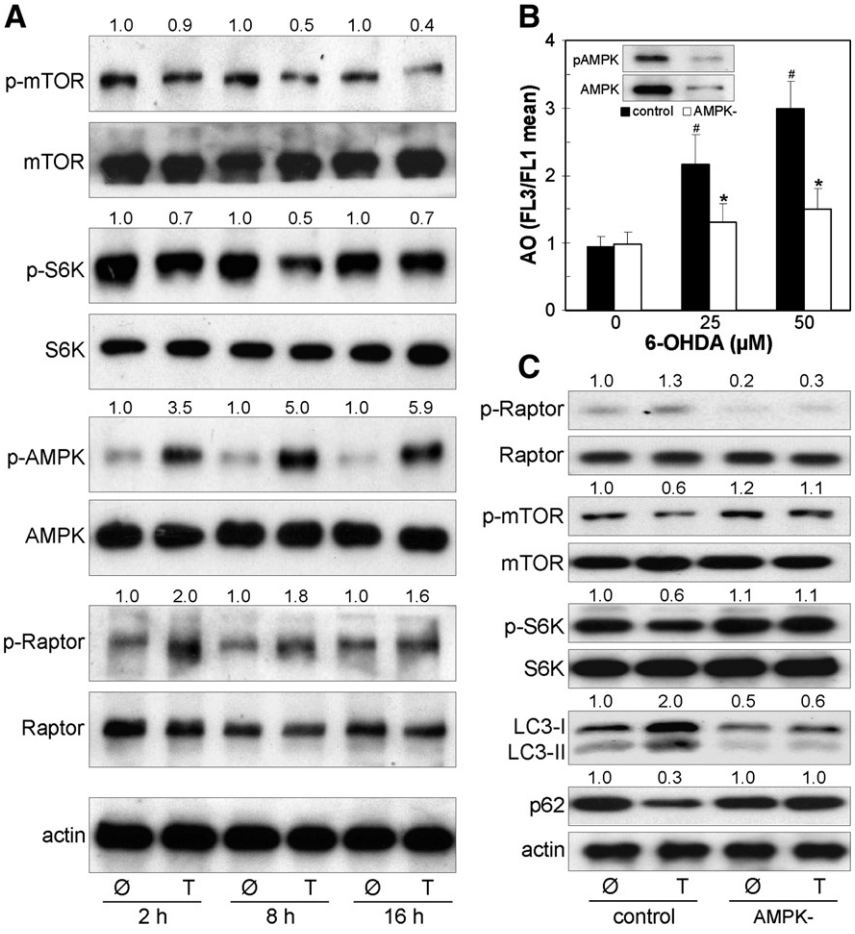

Fig. 3. 6-OHDA induced autophagy is associated with modulation of AMPK/mTOR signaling. (A) SH-SY5Y cells were incubated with 6-OHDA (50 μM) and the activation of AMPK/mTOR signaling molecules was assessed by immunoblotting at the indicated time points. The blots from a representative of three experiments are presented with the densitometry data above the relevant bands. (B) Control shRNA- or AMPK shRNA-transfected cells were treated with 6-OHDA for 16 h and the intracellular acidification was analyzed by flow cytometry after acridine orange (AO) staining (the insert shows immunoblot confirmation of AMPK knockdown). The data are mean ± SD values from three independent experiments ($^{\#}p<0.05$ vs. untreated control; $^{*}p<0.05$ vs. 6-OHDA-treated control). (C) Control shRNA- or AMPK shRNA-transfected cells were treated with 6-OHDA (50 μM) for 8 h and the activation of AMPK/mTOR signaling molecules, LC3 conversion and p62 levels were assessed by immunoblotting. The blots from one of at least two experiments with similar results are presented with the densitometry data above the relevant bands.

like vesicles containing cellular material (Fig. 2E). These data clearly demonstrate that apoptosis coincides with autophagy in 6-OHDA-treated SH-SY5Y cells.

3.3. 6-OHDA induced autophagy depends on AMPK/mTOR signaling

To evaluate molecular mechanisms of 6-OHDA-mediated autophagy, we analyzed the activation status of the main members of autophagy-regulating AMPK/mTOR signaling pathway. The treatment with 6-OHDA led to an increase in phosphorylation of AMPK and its direct downstream target Raptor (Fig. 3A). The activation of AMPK/Raptor was associated with the reduced phosphorylation of the major autophagy repressor mTOR and its substrate S6K (Fig. 4A). The RNA interference-mediated knockdown of AMPK expression prevented 6-OHDA mediated activation of Raptor and subsequent mTOR/p70S6K inhibition, LC3 conversion, p62 degradation and intracellular acidification (Fig. 3B, C). These data indicate that AMPK-dependent mTOR inhibition is involved in oxidopamine-stimulated autophagy in SH-SY5Y cells.

3.4. AMPK-dependent autophagy is involved in 6-OHDA neurotoxicity

To determine the role of autophagy in 6-OHDA toxicity towards SH-SY5Y cells, we tested if the latter could be modulated by inhibition or induction of autophagy. Pharmacological inhibitors of autophagy, which block either class III phosphoinositide 3-kinase-dependent formation of autophagosomes (wortmannin, 3-methyl adenine) or formation/acidification of autolysosomes (bafilomycin A1, NH_4Cl, chloroquine) [29], all markedly diminished 6-OHDA induced cell damage (Fig. 4A, B). Accordingly, autophagy knock-down with LC3β shRNA, confirmed by flow cytometric analysis of

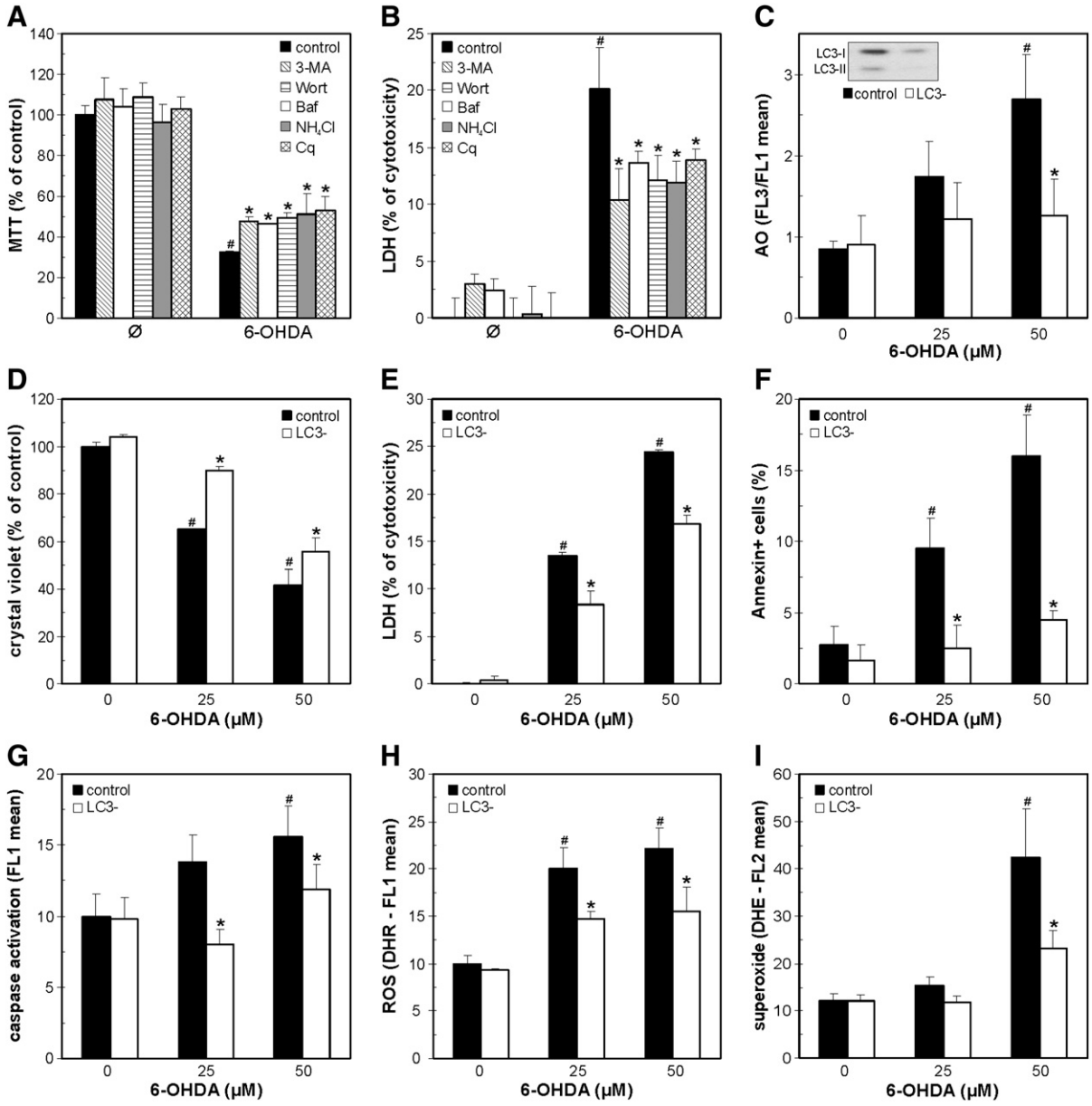

Fig. 4. Autophagy is involved in neurotoxicity of 6-OHDA. (A, B) SH-SY5Y cells were incubated with 6-OHDA (50 μM) in the presence or absence of the autophagy inhibitors 3-methyl adenine (3-MA; 4 mM), wortmannin (Wort; 100 nM), bafilomycin A1 (Baf; 2 nM), NH_4Cl (10 mM) and chloroquine (Cq; 20 μM). After 24 h, cell viability was assessed by MTT (A) and LDH release test (B). (C–I) SH-SY5Y cells transfected with control or LC3β shRNA were treated with 6-OHDA (the inset in C shows immunoblot verification of LC3β knockdown). Intracellular acidification (C), phosphatidylserine externalization (F), caspase activation (G), ROS production (H) or superoxide levels (I) were examined by flow cytometry after 16 h. Cell viability was assessed by crystal violet (D) and LDH release test (E) after 24 h. The data are mean ± SD values of triplicate measurements from a representative of three experiments (A, B, D, E) or mean ± SD values from three independent experiments (C, F–I) ($p^{\#}<0.05$ vs. untreated control; $^{*}p<0.05$ vs. 6-OHDA-treated control).

acridine orange red fluorescence and LC3 immunoblot (Fig. 4C), also significantly improved the viability of 6-OHDA-treated SH-SY5Y cells (Fig. 4D, E). The protective effects of autophagy knockdown in oxidopamine-treated neuroblastoma cells were associated with the reduction in phosphatidylserine externalization (Fig. 4F), caspase activation (Fig. 4G) and oxidative stress (Fig. 4H, I). Similar results were obtained in AMPK shRNA-transfected SH-SY5Y cells exposed to 6-OHDA, which displayed reduced cell death (Fig. 5A, B), phosphatidylserine externalization (Fig. 5C), caspase activation (Fig. 5D) and oxidative stress (Fig. 5E) in response to 6-OHDA. It should be noted that, in accordance with the previous findings [31], AMPK-deficient cells displayed reduced proliferation rate, but the difference was not significant after 24 h. In contrast to AMPK knockdown, a well-known mTOR inhibitor and autophagy inducer rapamycin [32] significantly increased 6-OHDA-induced death of SH-SY5Y cells (Fig. 5F), indicating a role for mTOR inhibition in cytotoxic autophagy triggered by the neurotoxin. Therefore, it appears that the AMPK/mTOR-dependent induction of autophagy is involved in apoptotic demise of SH-SY5Y cells upon oxidopamine treatment.

3.5. AMPK-dependent p38 activation mediates 6-OHDA neurotoxicity independently of autophagy

Considering the important role of mitogen-activated protein kinase (MAPK) family member p38 in 6-OHDA induced neurotoxicity [33], as well as in autophagy induction by various agents [34,35], we next investigated if p38 MAPK is involved in oxidopamine stimulated cytotoxic autophagy in SH-SY5Y cells. The treatment with 6-OHDA markedly

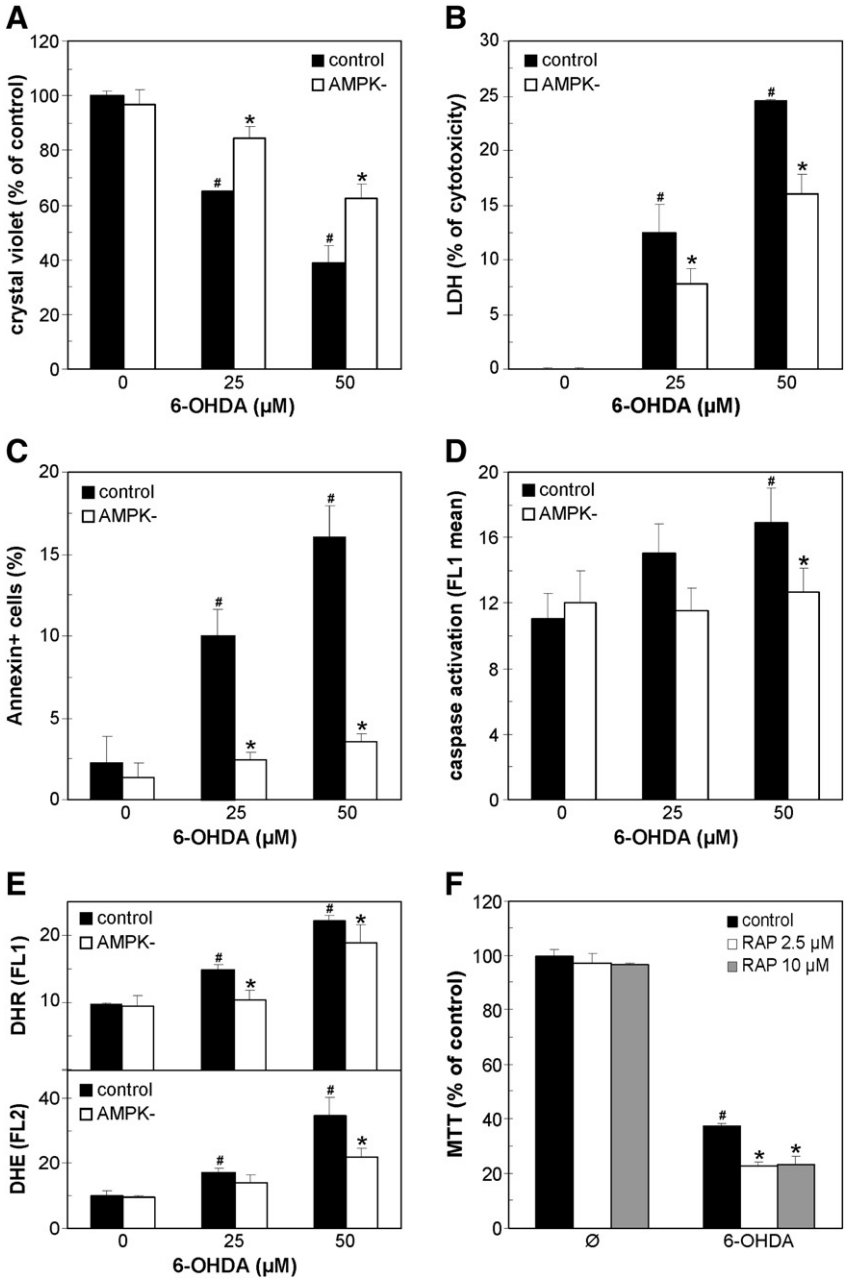

Fig. 5. AMPK/mTOR signaling is involved in neurotoxicity of 6-OHDA. (A–E) Control shRNA- or AMPK shRNA-transfected SH-SY5Y cells were treated with 6-OHDA and the cell viability was assessed by crystal violet (A) or LDH test (B) after 24 h. Phosphatidylserine externalization (C), caspase activation (D) and ROS or superoxide production (E) were examined by flow cytometry after 16 h. (F) SH-SY5Y cells were incubated with 6-OHDA (50 μM) in the presence or absence of rapamycin (RAP) and the cell viability was determined by MTT test after 24 h. The data are mean ± SD values of triplicate measurements from a representative of three experiments (A, B, F) or mean ± SD values from three independent experiments (C–E) ($p^{\#}<0.05$ vs. untreated control; $^{*}p<0.05$ vs. 6-OHDA-treated control).

stimulated the phosphorylation of p38 in both control and LC3$^-$ SH-SY5Y cells, but not in AMPK-deficient cells (Fig. 6A–C), despite the similar efficiency of LC3 and AMPK knockdown (approx. 70% — not shown). SB203580, the pharmacological p38 inhibitor that blocks its activity, but not phosphorylation [36], significantly reduced oxidopamine-induced neuroblastoma cell killing (Fig. 6E, F). Treatment with SB203580 had no effect on AMPK activity and LC3 conversion in 6-OHDA-exposed cells (Fig. 6D). Therefore, it seems that AMPK-mediated activation of p38 MAPK contributes to the 6-OHDA neurotoxicity in an autophagy-independent manner.

3.6. Oxidative stress is responsible for AMPK-mediated cytotoxic autophagy and p38 activation

Oxidative stress has been implicated in 6-OHDA induced p38 activation and subsequent neurotoxicity [37], as well as in AMPK phosphorylation in dopamine-treated neurons [38]. Accordingly, the antioxidant N-acetyl cysteine, which efficiently reduced ROS production (Fig. 7A), partly rescued neuroblastoma cells from 6-OHDA induced cytotoxicity (Fig. 7B). In addition, NAC prevented oxidopamine-stimulated activation of AMPK and p38 MAP kinase (Fig. 7C). Finally, oxidative stress was involved in autophagy induction, as NAC reduced 6-OHDA-stimulated LC3 conversion and intracellular acidification (Fig. 7C, D). These data indicate that oxidative stress is involved in oxidopamine-mediated AMPK activation and subsequent induction of cytotoxic autophagy and p38 activation (Fig. 8).

4. Discussion

The present study demonstrates that neurotoxin 6-OHDA induces autophagy in SH-SY5Y neuroblastoma cells through the oxidative stress-dependent activation of intracellular energy sensor AMPK and subsequent inhibition of the main autophagy repressor mTOR (Fig. 8). Furthermore, we show that both AMPK-dependent autophagy, as well as AMPK-mediated autophagy-unrelated p38 MAPK activation contribute to in vitro neurotoxicity of 6-OHDA (Fig. 8).

We assessed various autophagy endpoints, including LC3 conversion, autophagosome and autolysosome formation, cytoplasmic acidification and p62 degradation, to demonstrate the induction of autophagic response in neuroblastoma cells exposed to 6-OHDA. This is consistent with the several recent studies that reported the ability of oxidopamine to trigger autophagy in mouse and rat dopaminergic neurons [25–27] or human neuroblastoma cells [24]. While it has previously been shown that the induction of neuronal autophagy by 6-OHDA precursor dopamine was associated with AMPK activation [38], no direct evidence was provided for the involvement of AMPK in the observed autophagic response. By combining RNA interference and pharmacological approach, we here confirm that 6-OHDA-induced autophagy in human neuroblastoma cells depends on the activation of AMPK/Raptor and consequent inhibition of the negative autophagy regulator mTOR. The expression of the proautophagic protein beclin-1 was only marginally increased by 6-OHDA, consistent with the findings that mTOR inhibition-mediated autophagy can be beclin-independent [39]. Having in mind that the activation of extracellular signal-regulated kinase (ERK) has been implicated in autophagy induction by dopamine and neurotoxins 6-OHDA and MPP+ [24,40], we are currently investigating a possible interplay between ERK and AMPK signaling in this process.

In accordance with the view that autophagy can promote apoptosis in certain conditions [41,42], we here demonstrate that AMPK/mTOR-dependent autophagy is partly responsible for the induction of oxidative stress leading to caspase activation and apoptotic death in SH-SY5Y cells. To avoid possible off-target effects associated with the autophagy-modulating strategies [30], we have used several pharmacological inhibitors that block either early (autophagosome formation) or late (autolysosome formation) steps of the autophagic response, RNA interference, as well as mTOR-blocking autophagy inducer rapamycin. While it is still possible that some of the observed effects of autophagy inhibitors, LC3 shRNA and rapamycin were autophagy-independent, our data strongly argue in favor of the autophagy involvement in 6-OHDA

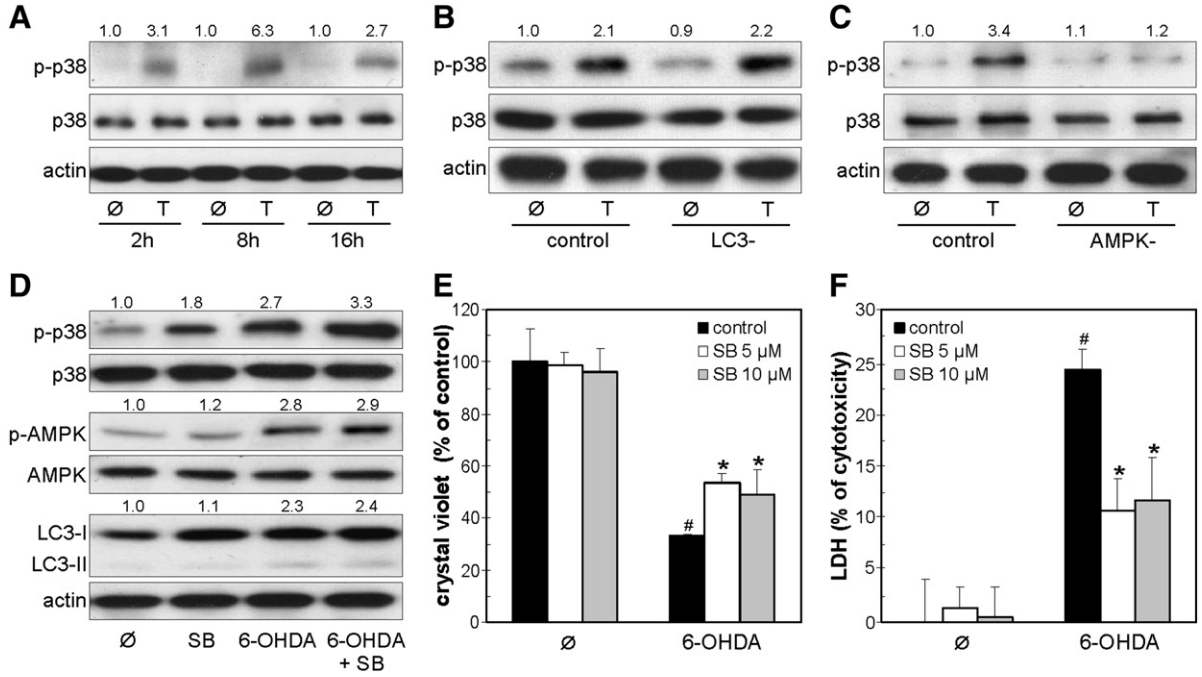

Fig. 6. AMPK/p38 signaling is involved in neurotoxicity of 6-OHDA. (A) SH-SY5Y cells were incubated with 6-OHDA (50 μM) and the phosphorylation of p38 was assessed by immunoblotting at the indicated time points. (B, C) SH-SY5Y cells transfected with control shRNA (B, C), LC3 shRNA (B) or AMPK shRNA (C) were treated with 6-OHDA (50 μM) for 8 h and p38 activation was determined by immunoblotting. (D–F) SH-SY5Y cells were incubated with 6-OHDA (50 μM) in the presence or absence of p38 inhibitor SB 203580 (10 μM). Phosphorylation of p38 and AMPK, as well as LC3 conversion were assessed by immunoblot after 8 h (D), while the cell viability was determined by crystal violet staining (E) and LDH test (F) after 24 h of incubation. The representative blots are presented with the densitometry data above the relevant bands, while the data in (E, F) are mean ± SD values of triplicate measurements from a representative of three experiments ($p^{\#}<0.05$ vs. untreated control; $^{*}p<0.05$ vs. 6-OHDA-treated control).

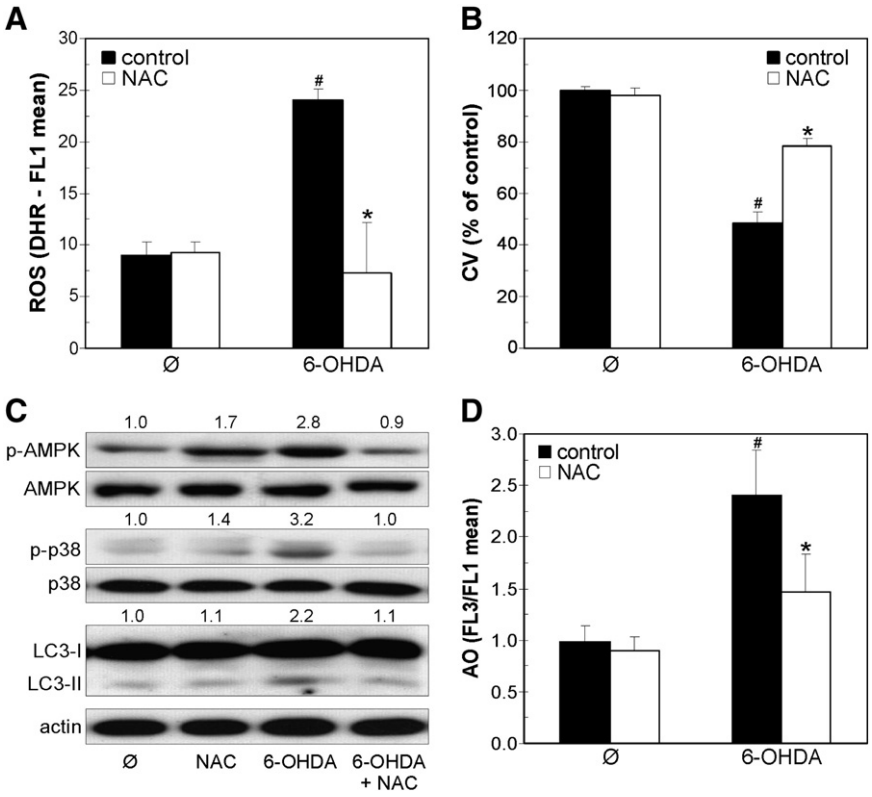

Fig. 7. 6-OHDA induced oxidative stress is involved in AMPK-mediated cytotoxic autophagy and p38 activation. (A–D) SH-SY5Y cells were stimulated with 6-OHDA (50 μM) in the presence or absence of N-acetyl cysteine (2 mM). After 16 h, ROS production following DHR staining (A) and cellular acidification in acridine orange (AO)-stained cells (D) were estimated by flow cytometry, while cell viability was determined by crystal violet test after 24 h (B). The data are mean ± SD values from three independent experiments (A, D) or mean ± SD values of triplicate measurements from a representative of three experiments (B) ($p^{\#}<0.05$ vs. untreated control; $^{*}p<0.05$ vs. 6-OHDA-treated control). (C) Phosphorylation of AMPK and p38, as well as LC3 conversion were assessed by immunoblot after 8 h. The representative blots are presented with the densitometry data above the relevant bands.

neurotoxicity. Accordingly, the previous in vivo studies have shown that the autophagy blocker 3-methyladenine or conditional deletion of the essential autophagy mediator Atg7 reduces 6-OHDA-triggered damage of dopaminergic neurons in rats or mice, respectively [25,27]. In the latter study, the neuroprotection was also achieved by enhancing the activity of Akt/mTOR signaling axis, thus indirectly suggesting that mTOR inhibition was involved in neurotoxic effects of autophagy [27]. Our data confirm and extend these findings by directly demonstrating the crucial role of AMPK as an upstream signal leading to the mTOR inhibition and subsequent induction of autophagy and cell death in oxidopamine-exposed neuronal cells. Interestingly, we have also observed that an autophagy-independent arm of AMPK signaling, involving p38 MAPK activation, could be involved in 6-OHDA neurotoxicity in vitro. This is in line with the ability of AMPK to stimulate p38 activation in different experimental settings [43,44], as well as with the known role of p38 in oxidopamine neurotoxic action [33,37]. On the other hand, unlike the results obtained here in 6-OHDA-exposed neuroblastoma cells, p38 MAPK contributed to autophagy induction in H_2O_2-treated fibroblasts or osteopontin-treated vascular smooth muscle cells [34,35], thus indicating a cell-specific and/or stimulus-specific effect.

Oxidative stress has a pivotal role in the induction of AMPK-dependent autophagy by dopamine [38]. Accordingly, we here demonstrated that oxidative stress was also responsible for the activation of AMPK and autophagy by 6-OHDA. Moreover, ROS production was responsible for AMPK-dependent phosphorylation of p38 MAP kinase in our study, indicating that previously reported involvement of oxidative stress in p38 activation by 6-OHDA [37] could at least partly rely on AMPK as an intermediate signal. Therefore, it seems that ROS production is both an effector mechanism of autophagic cell demise, as well as a very proximal event responsible for the initiation of AMPK-dependent autophagic response in 6-OHDA neurotoxicity. This is indeed consistent with the proposed involvement of 6-OHDA auto-oxidation products, monoamine oxidase-dependent H_2O_2 generation and delayed mitochondria-derived superoxide in the induction of oxidative stress and subsequent neuronal death [2,45].

Finally, it should be noted that only partial neuroprotection was achieved by inhibition of AMPK-dependent autophagy and p38 activation in our study, as well as by autophagy inhibition in vivo [25,27], indicating that some additional, AMPK-independent mechanisms, contribute to 6-OHDA neurotoxicity. There is also a question of the implications

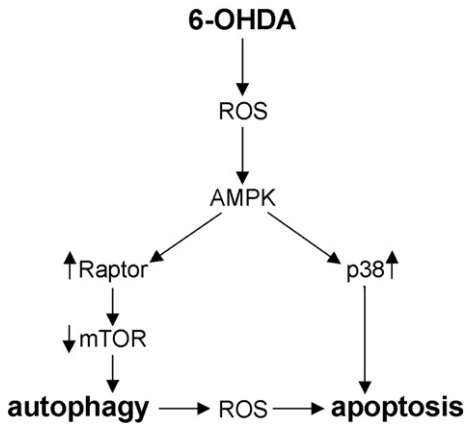

Fig. 8. A hypothetical model of the autophagy-dependent and -independent mechanisms of 6-OHDA neurotoxicity. Oxidative stress triggered by 6-OHDA causes activation of AMPK and subsequent mTOR inhibition-dependent induction of autophagy, which further promotes ROS production and contributes to apoptotic death of SH-SY5Y cells. On the other hand, AMPK-mediated increase in p38 MAPK activation contributes to apoptosis in an autophagy-independent manner.

that our findings may possibly have for the pathogenesis of PD. While the abnormal accumulation of autophagic vacuoles is evident in the brains of PD patients [39,46], the exact role of autophagy in PD is still unclear. The leading viewpoint is that autophagy may serve as a protective machinery for degradation of the accumulated α-synuclein and dysfunctional mitochondria [47], but evidence to the contrary exist [48]. This discrepancy could be timing-related, as it is conceivable that while autophagy might be beneficial as a clearing mechanism early in the pathological process, its excessive activation may be deleterious later on [49]. Thus, the model of neurotoxin-induced autophagic demise and here presented underlying mechanisms could be relevant for the latter situation, as well as for the investigation of other neuronal insults in which autophagy seems to play a destructive role [50].

In conclusion, the present report demonstrates that both autophagy-dependent and -independent mechanisms are involved in the in vitro neurotoxicity of oxidopamine. Both mechanisms are apparently controlled by oxidative stress-activated AMPK, involving mTOR inhibition in the former, and p38 MAPK activation in the latter neurotoxic pathway. Therefore, AMPK-mediated autophagy and p38 activation might be valid therapeutic targets for fighting neurodegeneration and neurotoxicity.

Acknowledgements

The study was supported by the Ministry of Science and Technological Development of the Republic of Serbia (grant numbers 173053 and 41025). Ljubica Harhaji-Trajkovic is a recipient of the UNESCO L'OREAL national scholarship program "For Women in Science".

References

[1] T. Klockgether, Parkinson's disease: clinical aspects, Cell Tissue Res. 318 (2004) 115–120.
[2] D. Blum, S. Torch, N. Lambeng, M. Nissou, A.L. Benabid, R. Sadoul, J.M. Verna, Molecular pathways involved in the neurotoxicity of 6-OHDA, dopamine and MPTP: contribution to the apoptotic theory in Parkinson's disease, Prog. Neurobiol. 65 (2001) 135–172.
[3] S. Senoh, C.R. Creveling, S. Udenfriend, B. Witkop, Chemical, enzymatic and metabolic studies on the mechanism of oxidation of dopamine, J. Am. Chem. Soc. 81 (1959) 6236–6240.
[4] H.C. Curtius, M. Wolfensberger, B. Steinmann, U. Redweik, J. Siegfried, Mass fragmentography of dopamine and 6-hydroxydopamine. Application to the determination of dopamine in human brain biopsies from the caudate nucleus, J. Chromatogr. 99 (1974) 529–540.
[5] G. Cohen, R.E. Heikkila, The generation of hydrogen peroxide, superoxide radical, and hydroxyl radical by 6-hydroxydopamine, dialuric acid, and related cytotoxic agents, J. Biol. Chem. 249 (1974) 2447–2452.
[6] T. Yorimitsu, D.J. Klionsky, Autophagy: molecular machinery for self-eating, Cell Death Differ. 12 (2005) 1542–1552.
[7] E. White, Autophagic cell death unraveled: pharmacological inhibition of apoptosis and autophagy enables necrosis, Autophagy 4 (2008) 399–401.
[8] S. Ghavami, A. Asoodeh, T. Klonisch, A.J. Halayko, K. Kadkhoda, T.J. Kroczak, S.B. Gibson, E.P. Booy, H. Naderi-Manesh, M. Los, Brevinin-2R(1) semi-selectively kills cancer cells by a distinct mechanism, which involves the lysosomal-mitochondrial death pathway, J. Cell. Mol. Med. 12 (2008) 1005–1022.
[9] S. Ghavami, M. Eshragi, S.R. Ande, W.J. Chazin, T. Klonisch, A.J. Halayko, K.D. McNeill, M. Hashemi, C. Kerkhoff, M. Los, S100A8/A9 induces autophagy and apoptosis via ROS-mediated cross-talk between mitochondria and lysosomes that involves BNIP3, Cell Res. 20 (2010) 314–331.
[10] P. Maycotte, A. Thorburn, Autophagy and cancer therapy, Cancer Biol. Ther. 11 (2011) 127–137.
[11] Y. Batlevi, A.R. La Spada, Mitochondrial autophagy in neural function, neurodegenerative disease, neuron cell death, and aging, Neurobiol. Dis. 43 (2011) 46–51.
[12] J.A. Lee, Neuronal autophagy: a housekeeper or a fighter in neuronal cell survival? Exp. Neurobiol. 21 (2012) 1–8.
[13] C. He, D.J. Klionsky, Regulation mechanisms and signaling pathways of autophagy, Annu. Rev. Genet. 43 (2009) 67–93.
[14] A.J. Meijer, P. Codogno, Regulation and role of autophagy in mammalian cells, Int. J. Biochem. Cell Biol. 36 (2004) 2445–2462.
[15] B.B. Kahn, T. Alquier, D. Carling, D.G. Hardie, AMP-activated protein kinase: ancient energy gauge provides clues to modern understanding of metabolism, Cell Metab. 1 (2005) 15–25.
[16] R.J. Shaw, LKB1 and AMP-activated protein kinase control of mTOR signalling and growth, Acta Physiol. 196 (2009) 65–80.
[17] Z.X. Xu, J. Liang, V. Haridas, A. Gaikwad, F.P. Connolly, G.B. Mills, J.U. Gutterman, A plant triterpenoid, avicin D, induces autophagy by activation of AMP-activated protein kinase, Cell Death Differ. 14 (2007) 1948–1957.
[18] A.L. Papandreou, K. Lim, N.C. Laderoute, Denko, Hypoxia signals autophagy in tumor cells via AMPK activity, independent of HIF-1, BNIP3, and BNIP3L, Cell Death Differ. 15 (2008) 1572–1581.
[19] L. Harhaji-Trajkovic, U. Vilimanovich, T. Kravic-Stevovic, V. Bumbasirevic, V. Trajkovic, AMPK-mediated autophagy inhibits apoptosis in cisplatin-treated tumour cells, J. Cell. Mol. Med. 13 (2009) 3644–3654.
[20] G. Filomeni, E. Desideri, S. Cardaci, I. Graziani, S. Piccirillo, G. Rotilio, M.R. Ciriolo, Carcinoma cells activate AMP-activated protein kinase-dependent autophagy as survival response to kaempferol-mediated energetic impairment, Autophagy 6 (2010) 202–216.
[21] V. Vingtdeux, L. Giliberto, H. Zhao, P. Chandakkar, Q. Wu, J.E. Simon, E.M. Janle, J. Lobo, M.G. Ferruzzi, P. Davies, P. Marambaud, AMP-activated protein kinase signaling activation by resveratrol modulates amyloid-beta peptide metabolism, J. Biol. Chem. 285 (2010) 9100–9113.
[22] Y. Nakatsu, Y. Kotake, N. Takai, S. Ohta, Involvement of autophagy via mammalian target of rapamycin (mTOR) inhibition in tributyltin-induced neuronal cell death, J. Toxicol. Sci. 35 (2010) 245–251.
[23] C. Marin, E. Aguilar, In vivo 6-OHDA-induced neurodegeneration and nigral autophagic markers expression, Neurochem. Int. 58 (2011) 521–526.
[24] R.K. Dagda, J. Zhu, S.M. Kulich, C.T. Chu, Mitochondrially localized ERK2 regulates mitophagy and autophagic cell stress: implications for Parkinson's disease, Autophagy 4 (2008) 770–782.
[25] L. Li, X. Wang, X. Fei, L. Xia, Z. Qin, Z. Liang, Parkinson's disease involves autophagy and abnormal distribution of cathepsin L, Neurosci. Lett. 489 (2011) 62–67.
[26] X.F. Fei, Z.H. Qin, B. Xiang, L.Y. Li, F. Han, K. Fukunaga, Z.Q. Liang, Olomoucine inhibits cathepsin L nuclear translocation, activates autophagy and attenuates toxicity of 6-hydroxydopamine, Brain Res. 1264 (2009) 85–97.
[27] H.C. Cheng, S.R. Kim, T.F. Oo, T. Kareva, O. Yarygina, M. Rzhetskaya, C. Wang, M. During, Z. Talloczy, K. Tanaka, M. Komatsu, K. Kobayashi, H. Okano, N. Kholodilov, R.E. Burke, Akt suppresses retrograde degeneration of dopaminergic axons by inhibition of macroautophagy, J. Neurosci. 31 (2011) 2125–2135.
[28] G.N. Kaludjerovic, D. Miljkovic, M. Momcilovic, V.M. Djinovic, M. Mostarica Stojkovic, T.J. Sabo, V. Trajkovic, Novel platinum(IV) complexes induce rapid tumor cell death in vitro, Int. J. Cancer 116 (2005) 479–486.
[29] N. Mizushima, T. Yoshimori, B. Levine, Methods in mammalian autophagy research, Cell 140 (2010) 313–326.
[30] Y. Ichimura, T. Kumanomidou, Y.S. Sou, T. Mizushima, J. Ezaki, T. Ueno, E. Kominami, T. Yamane, K. Tanaka, M. Komatsu, Structural basis for sorting mechanism of p62 in selective autophagy, J. Biol. Chem. 283 (2008) 22847–22857.
[31] M.M. Shaw, W.K. Gurr, R.J. McCrimmon, D.F. Schorderet, R.S. Sherwin, 5′ AMP-activated protein kinase alpha deficiency enhances stress-induced apoptosis in BHK and PC12 cells, J. Cell. Mol. Med. 11 (2007) 286–298.
[32] B. Caramés, A. Hasegawa, N. Taniguchi, S. Miyaki, F.J. Blanco, M. Lotz, Autophagy activation by rapamycin reduces severity of experimental osteoarthritis, Ann. Rheum. Dis. 71 (2012) 575–581.
[33] M. Gomez-Lazaro, M.F. Galindo, C.G. Concannon, M.F. Segura, F.J. Fernandez-Gomez, N. Llecha, J.X. Comella, J.H. Prehn, J. Jordan, 6-Hydroxydopamine activates the mitochondrial apoptosis pathway through p38 MAPK-mediated, p53-independent activation of Bax and PUMA, J. Neurochem. 104 (2008) 1599–1612.
[34] Y. Luo, P. Zou, J. Zou, J. Wang, D. Zhou, L. Liu, Autophagy regulates ROS-induced cellular senescence via p21 in a p38 MAPKα dependent manner, Exp. Gerontol. 46 (2011) 860–867.
[35] Y.H. Zheng, C. Tian, Y. Meng, Y.W. Qin, Y.H. Du, J. Du, H.H. Li, Osteopontin stimulates autophagy via integrin/CD44 and p38 MAPK signaling pathways in vascular smooth muscle cells, J. Cell. Physiol. 227 (2012) 127–135.
[36] S. Kumar, M.S. Jiang, J.L. Adams, J.C. Lee, Pyridinylimidazole compound SB 203580 inhibits the activity but not the activation of p38 mitogen-activated protein kinase, Biochem. Biophys. Res. Commun. 263 (1999) 825–831.
[37] W.S. Choi, D.S. Eom, B.S. Han, W.K. Kim, B.H. Han, E.J. Choi, T.H. Oh, G.J. Markelonis, J.W. Cho, Y.J. Oh, Phosphorylation of p38 MAPK induced by oxidative stress is linked to activation of both caspase-8- and -9-mediated apoptotic pathways in dopaminergic neurons, J. Biol. Chem. 279 (2004) 20451–20460.
[38] P. Giménez-Xavier, R. Francisco, A.F. Santidrián, J. Gil, S. Ambrosio, Effects of dopamine on LC3-II activation as a marker of autophagy in a neuroblastoma cell model, Neurotoxicology 30 (2009) 658–665.
[39] P. Gao, C. Bauvy, S. Souquère, G. Tonelli, L. Liu, Y. Zhu, Z. Qiao, D. Bakula, T. Proikas-Cezanne, G. Pierron, P. Codogno, Q. Chen, M. Mehrpour, The Bcl-2 homology domain 3 mimetic gossypol induces both Beclin 1-dependent and Beclin 1-independent cytoprotective autophagy in cancer cells, J. Biol. Chem. 285 (2010) 25570–25581.
[40] J.H. Zhu, C. Horbinski, F. Guo, S. Watkins, Y. Uchiyama, C.T. Chu, Regulation of autophagy by extracellular signal-regulated protein kinases during 1-methyl-4-phenylpyridinium-induced cell death, Am. J. Pathol. 170 (2007) 75–86.
[41] M. Fimia, M. Piacentini, Toward the understanding of autophagy regulation and its interplay with cell death pathways, Cell Death Differ. 16 (2009) 933–934.
[42] M. Salazar, A. Carracedo, I.J. Salanueva, S. Hernández-Tiedra, M. Lorente, A. Egia, P. Vázquez, C. Blázquez, S. Torres, S. García, J. Nowak, G.M. Fimia, M. Piacentini, F. Cecconi, P.P. Pandolfi, L. González-Feria, J.L. Iovanna, M. Guzmán, P. Boya, G. Velasco, Cannabinoid action induces autophagy-mediated cell death through stimulation of ER stress in human glioma cells, J. Clin. Invest. 119 (2009) 1359–1372.
[43] C.H. Bae, J.W. Kim, S.B. Ye, S.Y. Song, Y.W. Kim, S.Y. Park, Y.D. Kim, AMPK induces MUC5B expression via p38 MAPK in NCI-H292 airway epithelial cells, Biochem. Biophys. Res. Commun. 409 (2011) 669–674.
[44] J.H. Kim, J.O. Lee, S.K. Lee, J.W. Moon, G.Y. You, S.J. Kim, S.H. Park, J.M. Park, S.Y. Lim, P.G. Suh, K.O. Uhm, M.S. Song, H.S. Kim, The glutamate agonist homocysteine

sulfinic acid stimulates glucose uptake through the calcium-dependent AMPK-p38 MAPK-protein kinase C zeta pathway in skeletal muscle cells, J. Biol. Chem. 286 (2011) 7567–7576.
[45] S.M. Kulich, C. Horbinski, M. Patel, C.T. Chu, 6-Hydroxydopamine induces mitochondrial ERK activation, Free Radic. Biol. Med. 43 (2007) 372–383.
[46] P. Anglade, S. Vyas, F. Javoy-Agid, M.T. Herrero, P.P. Michel, J. Marquez, A. Mouatt-Prigent, M. Ruberg, E.C. Hirsch, Y. Agid, Apoptosis and autophagy in nigral neurons of patients with Parkinson's disease, Histol. Histopathol. 12 (1997) 25–31.
[47] C.T. Chu, Diversity in the regulation of autophagy and mitophagy: lessons from Parkinson's disease, Parkinsons Dis. 2011 (2011) 789431.
[48] M. Xilouri, L. Stefanis, Autophagy in the central nervous system: implications for neurodegenerative disorders, CNS Neurol. Disord. Drug Targets 9 (2010) 701–719.
[49] M. Xilouri, L. Stefanis, Autophagic pathways in Parkinson disease and related disorders, Expert Rev. Mol. Med. 21 (13) (2011) e8.
[50] Y. Yang, K. Fukui, T. Koike, X. Zheng, Induction of autophagy in neurite degeneration of mouse superior cervical ganglion neurons, Eur. J. Neurosci. 26 (2007) 2979–2988.